Flow and heat transfer over a moving surface with non-linear velocity and variable thickness in a nanofluids in the presence of Brownian motion

CrossMark

M.S. Abdel-wahed [a],*, E.M.A. Elbashbeshy [b], T.G. Emam [b]

[a] Engineering Mathematics and Physics Department, Faculty of Engineering, Modern University-MTI, Cairo, Egypt
[b] Mathematics Department, Faculty of Science, Ain Shams University, Abbassia, Cairo, Egypt

A R T I C L E   I N F O

A B S T R A C T

The effects of variable thickness, hydromagnetic flow, Brownian motion, heat generation, on heat transfer characteristics and mechanical properties of a moving surface embedded into cooling medium consists of water with nano-particles are studied. The governing boundary layer equations are transformed to ordinary differential equations. These equations are solved analytically using (OHAM) for general conditions. The velocity, temperature, and concentration profiles within the boundary layer are plotted and discussed in details for various values of the different parameters such as Brownian parameter, thermophoresis parameter, shape parameter, magnetic parameter and heat source parameter the effect of the cooling medium and flatness on the mechanical properties of the surface are investigated.

1. Introduction

The problem of boundary layer flow over a moving surface into a cooling medium is a mathematical simulation to the heat treatment process. The process of heat-treating is the method by which metals heated and cooled in a series of specific operations that never allow the metal to reach the molten state. The purpose of heat-treating is to make a metal more useful by changing or restoring its mechanical properties. Through heat-treating, we can make a metal harder, stronger, and more resistant to impact. Heat-treating can also make a metal softer and more ductile.

The boundary layer flow caused by a moving surface has drawn the attention of many researches [1–17]. The dynamics of the boundary layer flow over a moving surface embedded into a regular fluid was the main goal of many researchers until the advent of new type of fluid, which called a nanofluid.

Nanofluid described as a fluid in which solid nanoparticles with the length scales of 1–100 nm suspended in conventional heat transfer basic fluid. These nanoparticles enhance thermal conductivity and convective heat transfer coefficient of the base fluid significantly. Conventional heat transfer fluids such as oil, water and ethylene glycol mixture are poor heat transfer fluids because the thermal conductivity affects the heat transfer coefficient between the heat transfer medium and the heat transfer surface. Therefore, numerous methods have been taken to improve the thermal conductivity of these fluids by suspending nano/micro sized particle materials in liquids. The term nanofluid has been suggested by Choi [18]. There are many

---

* Corresponding author.
  E-mail address: eng_moh_sayed@live.com (M.S. Abdel-wahed).

studies on the mechanism behind the enhanced heat transfer characteristics using nanofluids. The collection of papers on this topic is included in the book by Das et al. [19] and in the review papers by Azizah et al. [20], Aminreza et al. [21], Nazar et al. [22], Hamad [23], Oztop et al. [24], Yacob et al. [25], prasad [26], and Elbashbeshy et al. [27].

On the other hand, the effect of Brownian motion and thermophoresis of a nanofluid have been investigated by Rana [28], Alsaedi [29], Khan [30], and Anbuchezhian [31].

All of the previous studies deal with moving surface with constant thickness under different effects of flow and thermo boundary layer. The variable thickness may occur in the engineering applications more frequently than a flat surface. Fang et al. [32] studied the boundary layer flow over a stretching sheet with variable thickness. Elbashbeshy et al. [33] studied the flow and heat transfer over a moving surface with non-linear velocity and variable thickness in a nanofluid.

The objective of the present paper is to study the effect of hydro-magnetic flow and heat transfer characteristic of a nanofluid over a steady moving surface with variable thickness on the mechanical properties of the surface in the presence of Brownian motion and heat source during the heat-treating process.

2. Formulation of the problem

Consider a steady, laminar, two dimensional flow of an incompressible viscous electrically conduction nanofluid over a continuous moving surface in the presence of a transverse magnetic field $B(x)$ and heat generation $Q(x)$. We assume that the surface is sufficiently thin with no induced stream-wise pressure gradients and the induced magnetic field produced by the motion of an electrically conducting fluid is negligible. This assumption is valid for small magnetic Reynolds number. Further, since there is no external electric field, the electric field due to polarization of charges is negligible. Moreover, it is assumed that both the fluid phase and nanoparticles are in thermal equilibrium state and no slip occurs between them.

Fig. 1 shows the x-axis runs along the center of the surface, and the y-axis is perpendicular to it.

We assume that the surface is not flat with a given profile, which is specified as $y = \delta(x+b)^{\frac{1-n}{2}}$, we assume the coefficient δ being small so that the surface is sufficiently thin.

The governing boundary layer equations for the steady two-dimensional laminar hydro-magnetic nanofluid flow over a moving surface and subjected heat source can be written as

$$\frac{\partial u}{\partial x} + \frac{\partial v}{\partial y} = 0 \tag{1}$$

$$u\frac{\partial u}{\partial x} + v\frac{\partial u}{\partial y} = v\frac{\partial^2 u}{\partial y^2} - \frac{\sigma B^2(x)}{\rho}u \tag{2}$$

$$u\frac{\partial T}{\partial x} + v\frac{\partial T}{\partial y} = \alpha\frac{\partial^2 T}{\partial y^2} + \tau\left[D_B\frac{\partial C}{\partial y}\frac{\partial T}{\partial y} + \frac{D_T}{T_\infty}\left(\frac{\partial T}{\partial y}\right)^2\right] + \frac{Q(x)}{\rho Cp}(T - T_\infty) \tag{3}$$

$$u\frac{\partial C}{\partial x} + v\frac{\partial C}{\partial y} = D_B\frac{\partial^2 C}{\partial y^2} + \frac{D_T}{T_\infty}\left(\frac{\partial^2 T}{\partial y^2}\right) \tag{4}$$

With boundary conditions

$$\begin{aligned} u = U_w, \quad v = 0, \quad T = T_w, \quad C = C_w, \quad &\text{at } y = \delta(x+b)^{\frac{1-n}{2}} \\ u = 0, \quad v = 0, \quad T = T_\infty, \quad C = C_\infty \quad &\text{as } y \to \infty \end{aligned} \tag{5}$$

where u and v are velocity components in the x and y directions, respectively, υ is the kinematic viscosity, ρ is the density of the base fluid, σ is the electrical conductivity, and α is the thermal diffusion, D_B is the Brownian diffusion coefficient, D_T is the Thermophoretic diffusion coefficient, τ is the ratio between the effective heat capacity of the nanoparticle and heat capacity of the fluid, $B(x)$ is the strength of the magnetic field. The special form of the magnetic field $B(x) = B_0(x+b)^{\frac{n-1}{2}}$ and heat
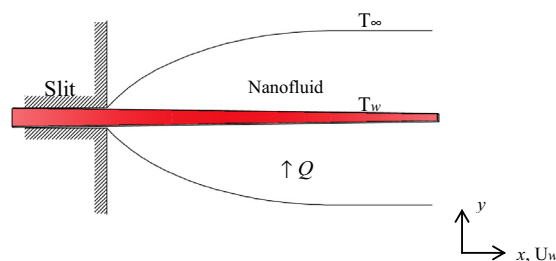

Fig. 1. Physical model and coordinate system.

generation $Q(x) = Q_0(x + b)^{n-1}$ are chosen to obtain a similarity solution. This form of $B(x)$ has also been considered by prasad [26].

The velocity, temperature, and the nanoparticle concentration are assumed in the form

$$U_{w(x)} = a(x + b)^n, \quad \theta(\eta) = \frac{T - T_\infty}{T_w - T_\infty}, \quad \phi(\eta) = \frac{C - C_\infty}{C_w - C_\infty} \tag{6}$$

where a and b are constants. n is the shape parameter. It is assumed $n > -1$ in this work for the validity of the similarity variable and functions.

3. Similarity transformation

We look for a similarity solution of Eqs. (1)–(4) subjected to the boundary conditions (5) of the following form

$$\eta = y\sqrt{\left(\frac{n+1}{2}\right)\left(\frac{a(x+b)^{n-1}}{\upsilon}\right)}, \quad \psi = \sqrt{\left(\frac{2}{n+1}\right)(x+b)^{n+1}a\upsilon}F(\eta) \tag{7}$$

where η is the similarity variable, and ψ is the stream function which is defined as $u = \frac{\partial\psi}{\partial y}$ and $\upsilon = -\frac{\partial\psi}{\partial x}$ which satisfies Eq. (1), substituting Eq. (7) into Eqs. (2)–(4), we obtain the following ordinary differential equations

$$F''' + FF'' - \left(\frac{2n}{n+1}\right)F'^2 - \left(\frac{2}{n+1}\right)MF' = 0 \tag{8}$$

$$\frac{1}{Pr}\theta'' + F\theta' + \left(\frac{2}{n+1}\right)\lambda\theta + Nb\theta'\phi' + Nt\theta'^2 = 0 \tag{9}$$

$$\phi'' + \frac{1}{2}LeF\phi' + \left(\frac{Nt}{Nb}\right)\theta'' = 0 \tag{10}$$

With boundary conditions

$$F(\alpha) = \alpha\left(\frac{1-n}{1+n}\right), \quad F'(\alpha) = 1, \quad \theta(0) = 1, \quad \phi(0) = 1 \quad \text{and} \quad F'(\infty) = 0, \quad \theta(\infty) = 0, \quad \phi(\infty) = 0 \tag{11}$$

here primes denote differentiation with respect to (η) where, $\alpha = \delta\sqrt{\frac{1+n}{2}\frac{a}{\upsilon}}$ is the surface thickness parameter and $\eta = \alpha = \delta\sqrt{\frac{1+n}{2}\frac{a}{\upsilon}}$ indicates the plate surface. We defined $F(\eta) = f(\eta - \alpha) = f(\zeta)$, Therefore the similarity Eqs. (8)–(10) and the associated boundary conditions (11) become

$$f''' + ff'' - \left(\frac{2n}{n+1}\right)f'^2 - \left(\frac{2}{n+1}\right)Mf' = 0 \tag{12}$$

$$\theta'' + Pr\left[f\theta' + \left(\frac{2}{n+1}\right)\lambda\theta + Nb\theta'\phi' + Nt\theta'^2\right] = 0 \tag{13}$$

$$\phi'' + \frac{1}{2}Lef\phi' + \left(\frac{Nt}{Nb}\right)\theta'' = 0 \tag{14}$$

With boundary conditions

$$f(0) = \alpha\left(\frac{1-n}{1+n}\right), \quad f'(0) = 1, \quad \theta(0) = 1, \quad \phi(0) = 1 \quad \text{and} \quad f'(\infty) = 0, \quad \theta(\infty) = 0, \quad \phi(\infty) = 0 \tag{15}$$

here primes denote differentiation with respect to (ζ), where

$$Pr = \frac{\upsilon}{\alpha}, \quad Le = \frac{\upsilon}{D_B}, \quad M = \frac{\beta_0^2\sigma}{a\rho}, \quad \lambda = \frac{Q_0}{a\rho Cp}, \quad Nb = \frac{\tau D_B}{\upsilon}(C_w - C_\infty), \quad Nt = \frac{\tau D_t}{\upsilon T_\infty}(T_w - T_\infty) \quad \text{and} \quad \tau = \frac{(\rho Cp)_p}{(\rho Cp)_f}$$

Here Pr, Le, M, λ, Nb, and Nt denote the Prandtl number, the Lewis number, magnetic field parameter, the heat source parameter, the Brownian motion parameter and the thermophoresis parameter respectively.

4. Analytical solution using optimal homotopy asymptotic method (OHAM)

In this section, the optimal homotopy asymptotic method is applied to nonlinear ordinary differential equations (12)–(14) with the boundary conditions (15) with the following assumptions

$$f = f_0 + pf_1 + p^2f_2, \quad \theta = \theta_0 + p\theta_1 + p^2\theta_2, \quad \phi = \phi_0 + p\phi_1 + p^2\phi_2, \quad H_1(p) = pC_1 + p^2C_2, \quad H_2(p)$$
$$= pC_3 + p^2C_4, \text{ and } H_3(p) = pC_5 + p^2C_6$$

where $p \in [0, 1]$ is an embedding parameter, H_p is a nonzero auxiliary function, C_i are constants [34].

4.1. Analytical solution of the momentum boundary layer problem

The optimal homotopy asymptotic method is applied to nonlinear ordinary differential equation (12) with the boundary conditions (15) under the following assumption

$$\mathcal{L} = f'' + f' \text{ and } \mathcal{N} = f''' + ff'' - \left(\frac{2n}{n+1}\right)f'^2 - \left(\frac{2}{n+1}\right)Mf' - f'' - f'$$

where L is a linear operator, $\mathcal{N}$ is a nonlinear operator, Therefore the OHAM family equation is

$$(1-p)[f'' + f'] = H_p\left[f''' + ff'' - \left(\frac{2n}{n+1}\right)f'^2 - \left(\frac{2}{n+1}\right)Mf'\right] \tag{16}$$

Collecting the same powers of p, and equating each coefficient of p to zero, we obtain a set of differential equations with boundary conditions.

Zero order equation p^0

$$f_0'' + f_0' = 0, \quad f_0(0) = \alpha\left(\frac{1-n}{1+n}\right), \quad f_0'(0) = 1 \tag{17}$$

First order equation p^1

$$f_1'' + f_1' = f_0'' + f_0' + C1\left[f_0''' + f_0f_0'' - \left(\frac{2n}{n+1}\right)f_0'^2 - \left[\left(\frac{2}{n+1}\right)M\right]f_0'\right], \quad f_1(0) = 0, \quad f_1'(0) = 0 \tag{18}$$

Second order equation p^2

$$\left\{\begin{array}{l} f_2'' + f_2' = f_1'' + f_1' + C1\left[f_1''' + f_0f_1'' + f_1f_0'' - \left(\frac{4n}{n+1}\right)f_0'f_1' - \left[\left(\frac{2}{n+1}\right)M\right]f_1'\right] \\ + C2\left[f_0''' + f_0f_0'' - \left(\frac{2n}{n+1}\right)f_0'^2 - \left[\left(\frac{2}{n+1}\right)M\right]f_0'\right], \quad f_2(0) = 0, \quad f_2'(0) = 0 \end{array}\right\} \tag{19}$$

Solving differential equations (17)–(19) with the boundary conditions, the General solution of (13) can be determined in the form:

$$f(\zeta) = f_0(\zeta) + f_1(\zeta) + f_2(\zeta) \tag{20}$$

The residual equation for the problem obtained in the form

$$\mathfrak{R}_1(\zeta, C_1, C_2) = \left[f'''(\zeta) + f(\zeta)f''(\zeta) - \left(\frac{2n}{n+1}\right)f'^2(\zeta) - \left(\left(\frac{2}{n+1}\right)M\right)f'(\zeta)\right] \tag{21}$$

The optimally unknown constant C1 and C2 can be obtained from the conditions

$$\frac{\partial J_1}{\partial C1} = \frac{\partial J_1}{\partial C2} = 0 \quad \text{where } J_1(C_i) = \int_0^\infty \mathfrak{R}_1^2(\zeta, C_i)d\zeta \tag{22}$$

4.2. Analytical solution of the thermal boundary layer problem

The optimal homotopy asymptotic method is applied to nonlinear ordinary differential equation (13) with the boundary conditions (15) under the following assumptions

$$\mathcal{L} = \theta' + \theta \text{ and } \mathcal{N} = \theta'' + P_r\left[f\theta' + \left(\frac{2}{n+1}\right)\lambda\theta + Nb\theta'\phi' + Nt\theta'^2\right] - \theta' - \theta$$

where L is a linear operator, $\mathcal{N}$ is a nonlinear operator, Therefore the OHAM family equation is

$$(1-p)[\theta' + \theta] = H_p\left[\theta'' + P_r\left[f\theta' + \left(\frac{2}{n+1}\right)\lambda\theta + Nb\theta'\phi' + Nt\theta'^2\right]\right] \tag{23}$$

Collecting the same powers of p, and equating each coefficient of p to zero, we obtain a set of differential equations with boundary conditions.

Zero order equation p^0

$$\theta_0' + \theta_0 = 0, \quad \theta_0(0) = 1 \tag{24}$$

First order equation p^1

$$\theta_1' + \theta_1 = \theta_0' + \theta_0 + C3\left[\theta_0'' + P_r\left[f_0\theta_0' + \left(\frac{2}{n+1}\right)\lambda\theta_0 + Nb\theta_0'\phi_0' + Nt\theta_0'^2\right]\right], \quad \theta_1(0) = 0 \tag{25}$$

Second order equation p^2

$$\left\{\begin{array}{c} \theta_2' + \theta_2 = \theta_1' + \theta_1 + C3\left[\theta_1'' + P_r\left[f_0\theta_1' + f_1\theta_0' + \left(\frac{2}{n+1}\right)\lambda\theta_1 + Nb\theta_0'\phi_1' + Nb\theta_1'\phi_0' + 2Nt\theta_0'\theta_1'\right]\right] \\ + C4\left[\theta_0'' + P_r\left[f_0\theta_0' + \left(\frac{2}{n+1}\right)\lambda\theta_0 + Nb\theta_0'\phi_0' + Nt\theta_0'^2\right]\right], \quad \theta_2(0) = 0 \end{array}\right\} \tag{26}$$

Solving differential equations (24)–(26) with the boundary conditions, the General solution of (13) can be determined in the form:

$$\theta(\zeta) = \theta_0(\zeta) + \theta_1(\zeta) + \theta_2(\zeta) \tag{27}$$

The residual equation for the problem obtained in the form

$$\Re_2(\zeta, C3, C4) = \theta''(\zeta) + Pr\left[f(\zeta)\theta'(\zeta) + \left(\frac{2}{n+1}\right)\lambda\theta(\zeta) + Nb\theta'(\zeta)\phi'(\zeta) + Nt\theta'^2(\zeta)\right] \tag{28}$$

The optimally unknown constant $C3$ and $C4$ can be obtained from the conditions

$$\frac{\partial J_2}{\partial C3} = \frac{\partial J_2}{\partial C4} = 0 \quad \text{where} \quad J_2(C_i) = \int_0^\infty \Re_2^2(\zeta, C_i)d\zeta \tag{29}$$

4.3. Analytical solution of the concentration boundary layer problem

The optimal homotopy asymptotic method is applied to nonlinear ordinary differential equation (14) with the boundary conditions (15) under the following assumptions

$$\mathcal{L} = \phi' + \phi \quad \text{and} \quad \mathcal{N} = \phi'' + \frac{1}{2}Lef\phi' + \frac{Nt}{Nb}\theta'' - \phi' - \phi$$

where L is a linear operator, $\mathcal{N}$ is a nonlinear operator, therefore the OHAM family equation is

$$(1-p)[\phi' + \phi] = H_p\left[\phi'' + \frac{1}{2}Lef\phi' + \frac{Nt}{Nb}\theta''\right] \tag{30}$$

Collecting the same powers of p, and equating each coefficient of p to zero, we obtain a set of differential equations with the boundary conditions.

Zero order equation p^0

$$\phi_0' + \phi_0 = 0, \quad \phi_0(0) = 1 \tag{31}$$

First order equation p^1

$$\phi_1' + \phi_1 = \phi_0' + \phi_0 + C5\left[\phi_0'' + \frac{1}{2}Lef_0\phi_0' + \frac{Nt}{Nb}\theta_0''\right], \quad \phi_1(0) = 0 \tag{32}$$

Second order equation p^2

$$\left\{\begin{array}{c} \phi_2' + \phi_2 = \phi_1' + \phi_1 + C5\left[\phi_1'' + \frac{1}{2}Lef_0\phi_1' + \frac{1}{2}Lef_1\phi_0' + \frac{Nt}{Nb}\theta_1''\right] \\ + C6\left[\phi_0'' + \frac{1}{2}Lef_0\phi_0' + \frac{Nt}{Nb}\theta_0''\right], \quad \phi_2(0) = 0 \end{array}\right\} \tag{33}$$

Solving differential equations (31)–(33) with the boundary conditions, the General solution of (14) can be determined in the form:

$$\phi(\zeta) = \phi_0(\zeta) + \phi_1(\zeta) + \phi_2(\zeta) \tag{34}$$

The residual equation for the problem obtained in the form

$$\Re_3(\zeta, C_5, C_6) = \left[\phi''(\zeta) + \frac{1}{2}Lef(\zeta)\phi'(\zeta) + \frac{Nt}{Nb}\theta''(\zeta)\right] \tag{35}$$

The optimally unknown constant $C5$ and $C6$ can be obtained from the conditions

$$\frac{\partial J_3}{\partial C5} = \frac{\partial J_3}{\partial C6} = 0 \quad \text{where} \quad J_3(C_i) = \int_0^\infty \Re_3^2(\zeta, C_i)d\zeta \tag{36}$$

To validate the analytic method (OHAM) used in this study, the results for $-f''(0)$ are compared with the numerical solution which reported in Fang et al. [31] see Table 1.

5. Results

From the engineering point of view, the most important characteristics of the flow are the skin friction coefficient, Nusselt number and Sherwood number, which indicate physically to surface shear stress, rate of heat transfer and rate of mass transfer respectively. These characteristics affect directly on the mechanical properties of the surface during heat treatment process, such that increasing the rate of heat transfer from the surface accelerates the cooling of the surface, which improve the hardness, stiffness and strength of the surface but on the other hand decrease the ductility of the surface and increase surface cracking.

5.1. Surface shear stress

$$\tau_w = \mu \left(\frac{\partial u}{\partial y} \right)_{y=\delta(x+b)^{\frac{1-n}{2}}} = \mu U_w \sqrt{\frac{a}{\upsilon} \left(\frac{n+1}{2} \right) (x+b)^{n-1}} f''(0) \tag{37}$$

Since the skin friction coefficient given by

$$C_f = \frac{2\tau_w}{\rho U_w^2} \quad \text{i.e.} \quad 2\sqrt{\left(\frac{n+1}{2} \right)} f''(0) = \sqrt{R_e} C_{fx} \tag{38}$$

5.2. Surface heat flux (rate of heat transfer)

$$q_w = -k \left(\frac{\partial T}{\partial y} \right)_{y=\delta(x+b)^{\frac{1-n}{2}}} = -k(T_w - T_\infty) \sqrt{\left(\frac{n+1}{2} \right) \frac{a}{\upsilon}} (x+b)^{\frac{n-1}{2}} \theta'(0) \tag{39}$$

Since the Nusselt number given by

$$Nu = \frac{(x+b)q_w}{k(T_w - T_\infty)} \quad \text{i.e.} \quad \frac{Nu}{\sqrt{R_e}} = -\sqrt{\frac{n+1}{2}} \theta'(0) \tag{40}$$

5.3. Surface mass flux (rate of mass transfer)

$$q_m = -D_B \left(\frac{\partial C}{\partial y} \right)_{y=\delta(x+b)^{\frac{1-n}{2}}} = -D_B(C_w - C_\infty) \sqrt{\left(\frac{n+1}{2} \right) \frac{a}{\upsilon}} (x+b)^{\frac{n-1}{2}} \phi'(0) \tag{41}$$

Since the Sherwood number given by

$$Sh = \frac{(x+b)q_m}{D_B(C_w - C_\infty)} \quad \text{i.e.} \quad \frac{Sh}{\sqrt{R_e}} = -\sqrt{\frac{n+1}{2}} \phi'(0) \tag{42}$$

6. Discussions

We present in this study a mathematical simulation to the heat treatment process of a moving continuous surface with variable thickness using nanofluid as a cooling medium. The influence of all embedded parameters on the velocity, temperature and nanoparticles concentration within the boundary layer shown in Figs. 2–15. The Prandlt number of the base fluid (water) is kept constant at 7.

Table 1
The values of $-f''(0)$ at different values of n and α.

α	n	Fang et al. [32]	OHAM
0.25	0.50	0.93380	0.92641
	1.00	1.00000	1.00000
	5.00	1.11860	1.12623
0.5	0.50	0.97990	0.96335
	1.00	1.00000	1.00000
	2.00	1.02340	1.03339

Moreover, Tables 2–6 show the effect of all embedded parameters on the velocity gradient, temperature gradient and concentration gradient at the surface and the corresponding values of skin friction, Nusselt number and Sherwood number at $Re = 5 \times 10^5$.

6.1. Analysis of shape parameter (n)

Mainly the study depend upon the shape parameter or motion parameter (n) due to its importance, such that this parameter can controls the surface shape, type of motion and the behavior of the boundary layer.

One can observe that the outer shape of the surface depend on the value of n. such that for $n = 1$, the study reduced to flat surface with constant thickness while for $n < 1$, the study transformed to surface with increasing thickness and convex outer shape. However, for $n > 1$, the study transformed to surface with decreasing thickness and concave outer shape.

On the other hand, this parameter can also controls the type of motion such that for $n = 0$, the motion reduced to linear with constant velocity and the motion reduced to deceleration motion if $n < 1$ and acceleration motion for $n > 1$.

In addition, this parameter controls the normal boundary layer behavior such that for $n = 1$ the boundary condition (15) reduced to $f(0) = 0$ which indicates to impermeable surface. While for $n < 1$ the boundary condition becomes $f(0) > 0$ which indicates to suction process. Also for $n > 1$ the boundary condition becomes $f(0) < 0$ which indicates to injection process.

The effect of shape parameter on the velocity, temperature, and nanoparticles concentration shown in Figs. 2–4 respectively. It observed that increasing of n leads to increasing of the boundary layer velocity, and temperature but the nanoparticles concentration has reverse mechanism such that the increasing of n leads to decreasing of the nanoparticles concentration near the surface. Moreover, one can observe that by increasing of n the concentration layer near the surface increased.

On the other hand, the effect of shape parameter on the velocity gradient, temperature gradient, concentration gradient and the corresponding values of skin friction, Nusselt number and Sherwood number presented in Tables 2 and 3.

One can observe that the value of velocity gradient, temperature gradient and concentration gradient all decrease with increase of shape parameter n. Moreover, the increasing of n leads to increasing of surface skin friction and decreasing of Nusselt number and Sherwood number. Therefore, the rate of heat and mass transfer from the surface will be decreases. It is worth mentioning that decreases the rate of heat transfer from the surface leads to deceleration of cooling process, which has a direct negative effect on the mechanical properties of the surface such as hardness, stiffness, strength, etc.

6.2. Analysis of thickness parameter (α)

The effect of thickness parameter on the velocity, temperature, and nanoparticles concentration shown in Figs. 5–7 respectively. It is observed that increasing of α leads to decreasing of the velocity and temperature but the nanoparticles concentration has reverse mechanism such that the increasing of α leads to increasing of the nanoparticles concentration near the surface and decreasing far of it.

On the other hand, the effect of thickness parameter on the velocity gradient, temperature gradient, and the concentration gradient and the corresponding values of skin friction, Nusselt number and Sherwood number presented in Tables 2 and 3. It noted that the increasing of thickness parameter leads to increasing of all previous physical properties.

It is worth mentioning that increases the rate of heat transfer from the surface leads to acceleration of cooling process, which has a direct positive effect on the mechanical properties of the surface such as hardness, stiffness, strength.
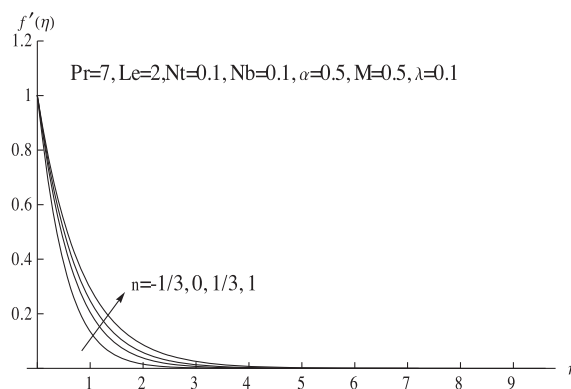
Fig. 2. The velocity profiles with increasing of shape parameter (n).

Table 2
Values of velocity gradient, temperature gradient and concentration gradient at the surface and the corresponding values of skin friction, Nusselt number and Sherwood number at $M = 0$, $Le = 2$, $Pr = 6.2$, $\lambda = Nt = Nb = 0.1$.

α	n	$f''(0)$	$\theta'(0)$	$\phi'(0)$	Cfx	Nu	Sh
0.5	−0.5	−1.166667	−9.186514	7.241713	−0.00165	3247.92	−2560.33
	0.50	−1.023235	−1.992730	1.122908	−0.00251	1220.29	−687.640
	1.00	−1.000000	−1.308134	0.479281	−0.00283	924.990	−338.900
1	−0.5	−2.833333	−18.314577	15.115865	−0.00401	6475.18	−5344.27
	0.50	−1.153874	−2.815158	1.888074	−0.00283	1723.93	−1156.20
	1.00	−1.000001	−1.308130	0.479266	−0.00283	924.990	−338.890

Table 3
Values of velocity gradient, temperature gradient and concentration gradient at the surface and the corresponding values of skin friction, Nusselt number and Sherwood number at $M = 1$, $Le = 2$, $Pr = 6.2$, $\lambda = Nt = Nb = 0.1$.

α	n	$f''(0)$	$\theta'(0)$	$\phi'(0)$	Cfx	Nu	Sh
0.5	−0.5	−2.698243	−9.212846	7.432311	−0.00382	3257.23	−2627.72
	0.50	−1.541648	−1.922033	1.153334	−0.00378	1177.00	−706.270
	1.00	−1.414214	−1.255416	0.587011	−0.00400	887.71	−415.080
1	−0.5	−3.866086	−18.326942	15.172941	−0.00547	6479.55	−5364.44
	0.50	−1.633396	−2.749794	1.854783	−0.00400	1683.90	−1135.82
	1.00	−1.414214	−1.255409	0.586987	−0.00400	887.71	−415.06

Table 4
Values of temperature gradient and concentration gradient at the surface and the corresponding values of Nusselt number and Sherwood number at $\alpha = n = M = 0.5$, $Le = 2$, $Pr = 6.2$, $Nt = Nb = 0.1$.

λ	$\theta'(0)$	$\phi'(0)$	Nu	Sh
−0.50	−3.112363	2.232995	1100.39	−789.48
−0.30	−2.777494	1.906843	1161.91	−797.69
0.00	−2.181766	1.328482	1090.88	−664.24
0.30	−1.372622	0.548155	782.51	−312.50
0.50	−0.528105	−0.259352	323.40	158.82

Table 5
Values of temperature gradient and concentration gradient at the surface and the corresponding values of Nusselt number and Sherwood number at $\alpha = n = M = 0.5$, $Le = 2$, $Pr = 6.2$, $\lambda = Nb = 0.1$.

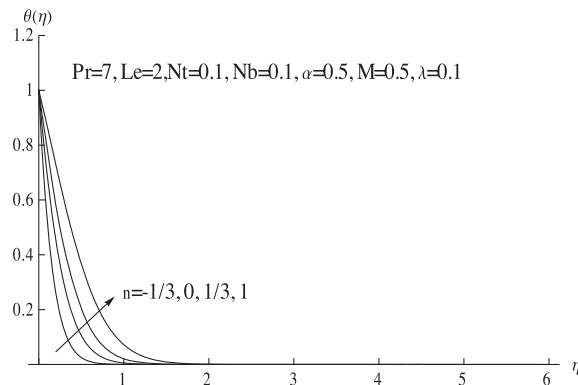| Nt	$\theta'(0)$	$\phi'(0)$	Nu	Sh
0.1	−1.945147	1.099440	1020.04	−576.55
0.3	−1.579208	3.374871	900.29	−1923.97
0.5	−1.269412	4.548747	777.35	−2785.53

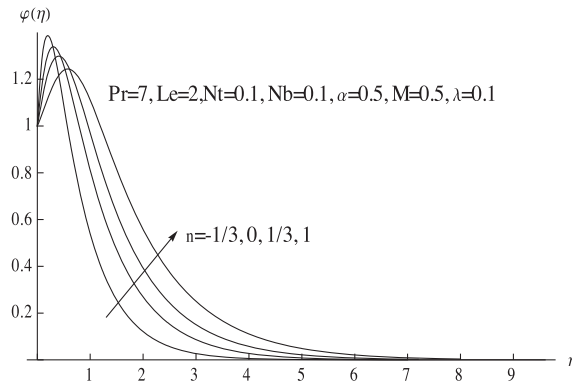**Fig. 3.** The temperature profiles with increasing of shape parameter (n).

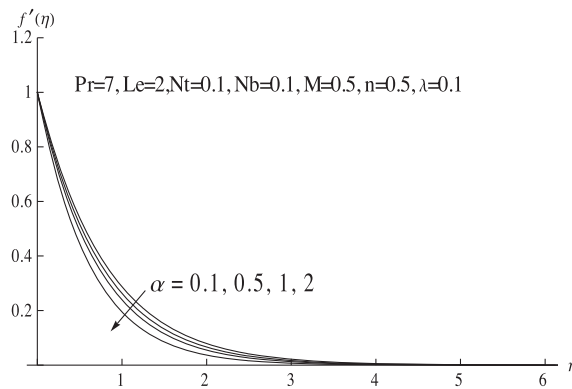**Fig. 4.** The concentration profiles with increasing of shape parameter (n).

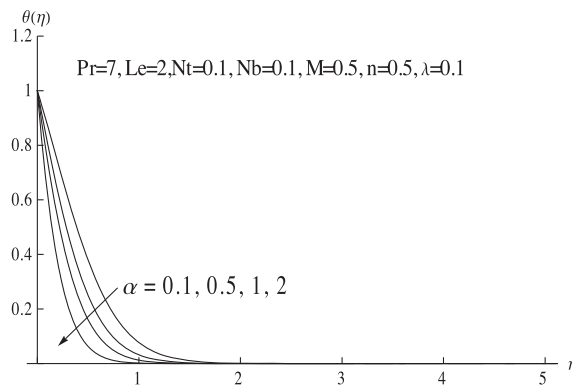**Fig. 5.** The velocity profiles with increasing of thickness parameter (α).

Fig. 6. The temperature profiles with increasing of thickness parameter (α).

6.3. Analysis of hydro-magnetic flow

The present study showed that the hydromagnetic flow has a direct impact on the boundary layer velocity and nanoparticles concentration through Figs. 8 and 9. Such that the increasing of magnetic parameter leads to decreasing of velocity and increasing of nanoparticles concentration.

On the other hand, the effect of hydromagnetic flow on the skin friction, Nusselt number and Sherwood number tabulated in Tables 2 and 3. By comparing between Tables 2 and 3, one can observe that using hydromagnetic flow as a cooling medium increase skin friction and Sherwood number but decrease Nusselt number by a limited values. Consequently, the surface shear stress and rate of mass transfer increased and rate of heat transfer decreased by increasing of magnetic parameter M.
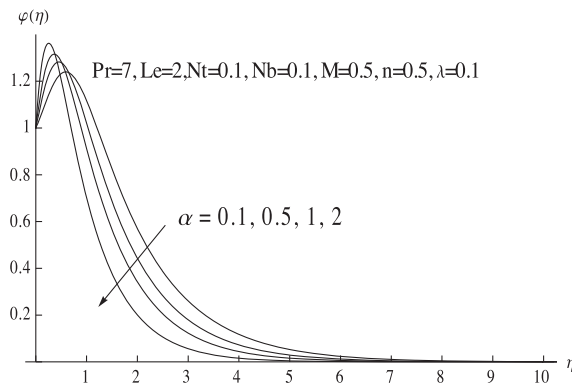
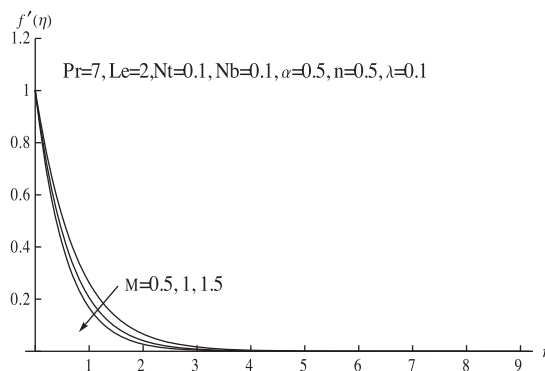**Fig. 7.** The concentration profiles with increasing of thickness parameter (α).

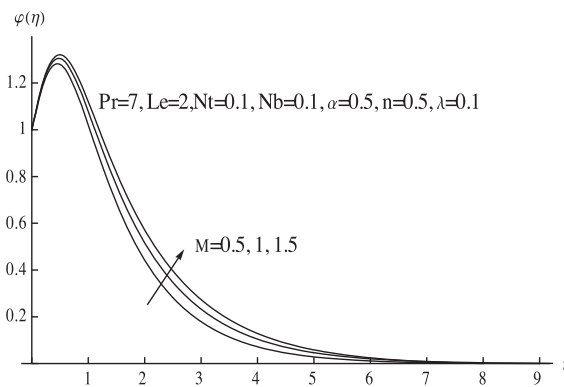**Fig. 8.** The velocity profiles with increasing of magnetic parameter (M).

Fig. 9. The concentration profiles with increasing of magnetic parameter (M).

6.4. Analysis of Brownian motion

Brownian motion is the random moving of particles suspended in a fluid (nanoparticles) resulting from their bombardment by the fast moving atoms or molecules in the fluid. This motion controls the temperature and the concentration of the particles within the boundary layer over the surface. The Brownian motion parameter Nb is the key of this mechanism such that the increasing of Nb leads to increasing of the boundary layer temperature and decreasing of the nanoparticles concentration as shown in Figs. 10 and 11. Moreover, one can observe that the profiles of nanoparticles concentration at $Nb = 0.3$ and $Nb = 0.5$ are very close but for $Nb = 0.1$ the concentration profile increased rapidly to a maximum level near the surface and decay gradually to zero, this profile indicates that the effect of Nb limited into a small range of its value. In addition,
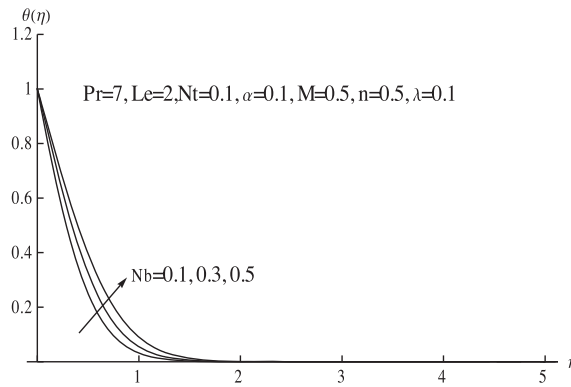
Fig. 10. The temperature profiles with increasing of Brownian parameter (*Nb*).
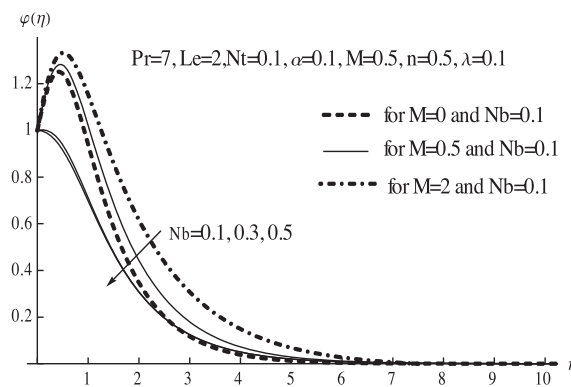

Fig. 11. The concentration profiles with increasing of Brownian parameter (*Nb*).

Fig. 11 shows that the concentration of the nanoparticles at $Nb = 0.1$ increases significantly in the presence of the hydromagnetic flow.

On the other hand, the effect of Brownian motion on the temperature gradient, concentration gradient and the corresponding values of Nusselt number, Sherwood number presented in Table 6. It is clear that this motion decrease the rate of heat and mass transfer by decreasing the Nusselt number, Sherwood number.

6.5. Analyses of thermophoresis particle deposition

Thermophoresis is a phenomenon observed in mixtures of mobile particles where the different particle types exhibit different responses to the force of a temperature gradient. Explain this phenomenon appears in this study through the thermophoresis parameter *Nt* such that increasing this parameter leads to increasing of boundary layer temperature and nanoparticles concentration as shown in Figs. 12 and 13. Moreover, Fig. 13 shows that increasing thermophoresis parameter from 0.1 to 0.5 leads to increasing of nanoparticles concentration near the surface to three times of its value.

It is worth mentioning that the thermophoresis parameter is possible to be a positive or negative signal such that the negative value of *Nt* indicates to hot surface while positive to cold surface. Moreover for hot surfaces, thermophoresis tends to blow the nanoparticles concentration boundary layer away from the surface since a hot surface repels the sub-micron sized particles from it, thereby forming a relatively particle free layer near the surface.

Table 6
Values of temperature gradient and concentration gradient at the surface at $\alpha = n = M = 0.5$, $Le = 2$, $Pr = 6.2$, $\lambda = Nt = 0.1$.

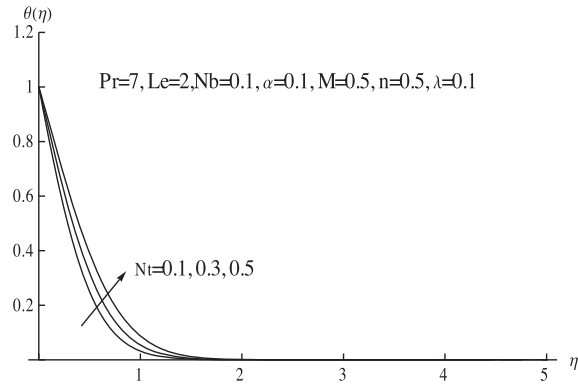| Nb	$\theta'(0)$	$\phi'(0)$	Nu	Sh
0.1	−1.945147	1.099440	1020.04	−576.55
0.3	−1.532260	0.037401	873.52	−21.322
0.5	−1.299666	−0.004258	795.88	2.6175

Fig. 12. The temperature profiles with increasing of thermophoresis parameter (Nt).
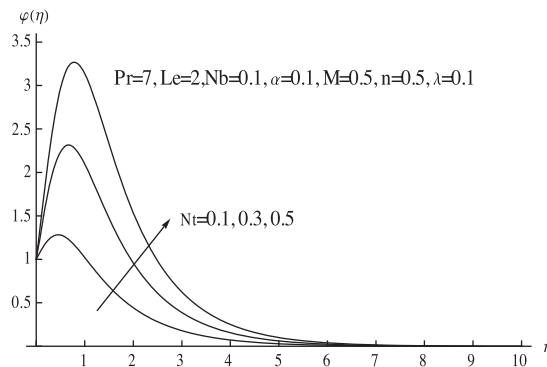

Fig. 13. The concentration profiles with increasing of thermophoresis parameter (Nt).
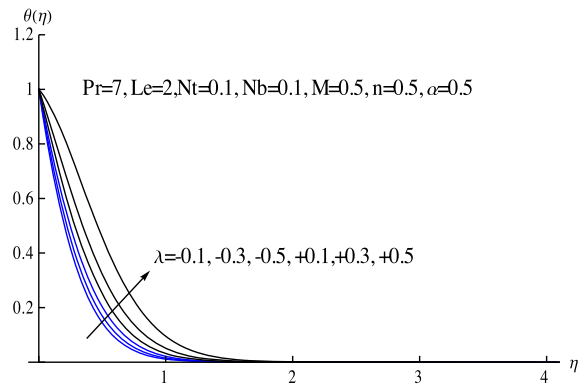

Fig. 14. The temperature profiles with increasing of heat source parameter (λ).

On the other hand, the effect of thermophoresis parameter on the temperature gradient, concentration gradient and the corresponding values of Nusselt number, Sherwood number shown in Table 5. It is clear that the increasing of thermophoresis parameter decreases the rate of heat transfer and increase mass transfer.

6.6. Analyses of heat source or sink

The effect of heat source parameter (λ) on the temperature and nanoparticles concentration showed in Figs. 14 and 15 respectively. As expected, the increasing of λ leads to increasing of boundary layer temperature and decreasing of
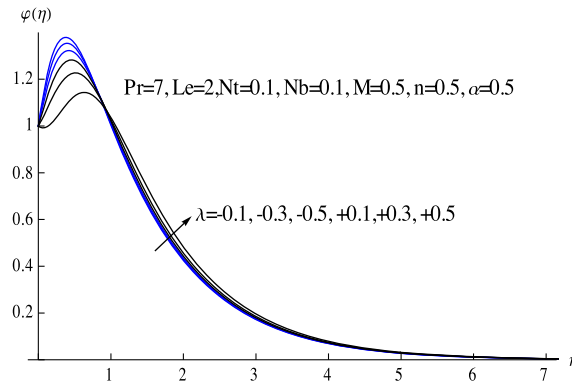
Fig. 15. The concentration profiles with increasing of heat source parameter (λ).

nanoparticles concentration close to the surface. Moreover, Table 4 shows the effect of this parameter on the temperature gradient, concentration gradient and the corresponding values of Nusselt number and Sherwood number. The results obtained in Table 4 indicates that the increasing of heat source parameter leads to decreasing of Nusselt number, Sherwood, heat and mass transfer from the surface.

7. Conclusions

We present in this study a mathematical model of a continuous moving surface with variable thickness embedded into a nanofluid. The heat and mass transfer characteristics and the mechanical properties of the surface were our goal in this study and the following results obtained:

- The flatness of the surface leads to boundary layer under suction or injection process according to the value of shape parameter.
- The flatness of the surface has a direct effect on the mechanical properties of the surface. (i.e. hardness, stiffness and strength). Such that the increasing of shape parameter n produces a negative effect on the surface mechanical properties.
- Using hydromagnetic flow as a cooling medium increase surface shear stress and rate of mass transfer from the surface and decrease the rate of heat transfer.
- The nanoparticle concentration near the non-flat surface is bigger and thinner than that on the flat surface.
- For all embedded parameters used in this study, the nanoparticles concentration profile increases rapidly near the surface and then return in decay.
- Effect of Brownian motion on the nanoparticles concentration increases in the presence of hydromagnetic flow.
- The Brownian motion and thermophoresis both have a negative effect on the surface hardness and strength.
- Boundary layer velocity increases with increase of shape parameter n and decrease of thickness parameter and magnetic field parameter.
- Boundary layer temperature increases with increase of shape parameter n, Brownian motion parameter, thermophoresis parameter, heat source parameter and decrease of thickness parameter.
- Nanoparticles concentration increases with decrease of shape parameter n, Brownian motion parameter, heat source parameter and increase of thickness parameter and magnetic field parameter and thermophoresis parameter.

References

[1] M.E. Ali, On thermal boundary layer on a power law stretched surface with suction or injection, Int. J. Heat Mass Flow 16 (1995) 280–290.
[2] E.M.A. Elbashbeshy, Heat transfer over a stretching surface with variable heat flux, J. Phys. D: Appl. Phys. 31 (1998) 1951–1955.
[3] E.M.A. Elbashbeshy, M.A.A. Bazid, The effect of temperature dependent viscosity on heat transfer over continuous moving surface, J. Phys. D: Appl. Phys. 33 (2000) 2721.
[4] E.M.A. Elbashbeshy, M.A.A. Bazid, Heat transfer in a porous medium over a stretching surface with internal heat generation and suction or injection, Appl. Math. Comput. 158 (3) (2004) 799–807.
[5] E.M.A. Elbashbeshy, M.A.A. Bazid, Heat transfer over a stretching surface with internal heat generation, Can. J. Phys. 81 (4) (2003) 699–703.
[6] E.M.A. Elbashbeshy, M.A.A. Bazid, Heat transfer over a continuously moving plate embedded in non-Darcian porous medium, Int. J. Heat Mass Transfer 43 (2000) 3087–3092.
[7] C.D.S. Devi, H.S. Takhar, G. Nath, Unsteady mixed convection flow in stagnation region adjacent to a vertical surface, Heat Mass Transfer 26 (1991) 71–79.
[8] H.T. Anderson, J.B. Aarsth, B.S. Dandapat, Heat transfer in a liquid film on an unsteady stretching surface, Int. J. Heat Transfer 43 (2000) 69–74.
[9] E.M.A. Elbashbeshy, M.A.A. Bazid, Heat transfer over an unsteady stretching surface, Heat Mass Transfer 41 (2004) 1–4.
[10] E.M.A. Elbashbeshy, M.A.A. Bazid, Heat transfer over an unsteady stretching surface with internal heat generation, Appl. Math. Comput. 138 (3) (2003) 239–245.

[11] R. Nazar, N. Amin, I. Pop, D. Flip, Unsteady boundary layer flow in the region of the stagnation point on a stretching sheet, Int. J. Eng. Sci. 42 (2004) 1241–1253.
[12] A. Ishak, R. Nazar, I. Pop, Heat transfer over an unsteady stretching permeable surface with prescribed wall temperature, Nonlinear Anal. Real World Appl. 10 (2009) 2909–2913.
[13] T.C. Chiam, Hydro magnetic flow over a surface stretching with a power-law velocity, Int. J. Eng. Sci. 33 (1995) 429–435.
[14] K. Vajravelu, Viscous flow over a nonlinearly stretching sheet, Appl. Math. Comput. 124 (2001) 281–288.
[15] K.V. Prasad, Dulal Pal, P.S. Datti, MHD power law fluid flow and heat transfer over a non-isothermal stretching sheet, Commun. Non-linear Sci. Numer. Simul. 14 (2009) 2178–2189.
[16] Rafael. Cortell, Effects of viscous dissipation and radiation on the thermal boundary layer over a nonlinearly stretching sheet, Phys. Lett. A 372 (2008) 631–636.
[17] K.V. Prasad, K. Vajravelu, P.S. Datti, The effects of variable fluid properties on the hydro-magnetic flow and heat transfer over a non-linearly stretching sheet, Int. J. Therm. Sci. 49 (2010) 603–610.
[18] S.U.S. Choi, Enhancing conductivity of fluids with nanoparticles, ASME Fluid Eng. Div. 231 (1995) 99–105.
[19] S.K. Das, S.U.S. Choi, W. Yu, T. Pradeep, Nanofluids: Science and Technology, Wiley, NJ, 2007.
[20] M. Azizah, A. Syakila, I. Pop, Flow and heat transfer over an unsteady shrinking sheet with suction in nanofluids, Int. J. Heat Mass Transfer 55 (2011) 1888–1897.
[21] N. Aminreza, P. Rashid, G. Mohamed, Effect of partial slip boundary condition on the flow and heat transfer of nanofluids past stretching sheet prescribed constant wall temperature, Int. J. Thermal Sci. (2012) 1–9
[22] R. Nazar, L. Tham, I. Pop, Mixed convection boundary layer flow from a horizontal circular cylinder embedded in a porous medium filled with a nanofluid, Transp. Porous Med. 86 (2011) 517–536.
[23] M. Hamad, Analytical solution of natural convection flow of a nanofluid over a linearly stretching sheet in the presence of magnetic field, Int. Commun. Heat Mass Transfer 38 (2011) 487–492.
[24] H.F. Oztop, E. Abu Nada, Numerical study of natural convection in partially heated rectangular enclosures filled with nanofluids, Int. J. Heat Fluid Flow 29 (2008) 1326–1336.
[25] N.A. Yacob, A. Ishak, R. Nazar, I. Pop, Boundary layer flow past a stretching/shrinking surface beneath an external uniform shear flow with a convective surface boundary condition in a nanofluid, Nanoscale Res. Lett. 6 (2011) 1–7.
[26] K.V. Prasad, K. Vajravelu, P.S. Datti, The Effect of variable fluid properties on the hydromagnetic flow and heat transfer over a non-linearly stretching sheet, Int. J. Therm. Sci. 49 (2010) 603–610.
[27] E.M.A. Elbashbeshy, T.G. Emam, M.S. Abde-wahed, Effect of magnetic field on flow and heat transfer of a nanofluid over an unsteady continuous moving surface in the presence of suction/injection, Int. J. Appl. Math. 14 (10) (2012) 436–442.
[28] P. Rana, R. Bhargava, Flow and heat transfer of a nanofluid over a nonlinearly stretching sheet, Commun. Nonlinear Sci. Numer. Simul. 17 (2012) 212–226.
[29] A. Alsaedi, M. Awais, T. Hayat, Effects of heat generation/absorption on stagnation point flow of nanofluid over a surface with convective boundary conditions, Commun. Nonlinear Sci. Numer. Simul. 17 (2012) 4210–4223.
[30] W.A. Khan, I. Pop, Boundary layer flow of a nanofluid past a stretching sheet, Int. J. Heat Mass Transfer 53 (2010) 2477–2483.
[31] N. Anbuchezhian, K. Srinivasan, K. Chandrasekaran, R. Kandasamy, Thermophoresis and Brownian motion effects on boundary layerflow of nanofluid in presence of thermal stratification due to solar energy, Appl. Math. Mech. 33 (2012) 765–780.
[32] Tiegang. Fang, Ji. Zhang, Yongfang. Zhong, Boundary layer flow over a stretching sheet with variable thickness, Appl. Math. Comput. 218 (2012) 7241–7252.
[33] E.M.A. Elbashbeshy, T.G. Emam, M.S. Abde-wahed, Flow and heat transfer over a moving surface with non-linear velocity and variable thickness in a nanofluid in the presence of thermal radiation, Can. J. Phys. 91 (2013) 699–708.
[34] V. Marinca, N. Herisanu, Application of optimal homotopy method for solving nonlinear equations arising in heat transfer, Int. Commun. Heat Mass Transfer 35 (2008) 710–715.